

# Doping dependence of chiral superconductivity in near 45° twisted bilayer cuprates

Mathieu Bélanger<sup>1</sup> and David Sénéchal<sup>1</sup>

<sup>1</sup>Département de physique and Institut quantique, Université de Sherbrooke, Sherbrooke, Québec, Canada J1K 2R1

(Dated: June 12, 2023)

We study a one-band Hubbard model for a twisted cuprate bilayer with a twist angle of 43.6° and a moire cell containing 58 sites. We use the variational cluster approximation (VCA), which treats short-range correlations exactly and leads, in single layers, to a dome of *d*-wave superconductivity away from half-filling from strong on-site repulsion alone. We find a time-reversal-symmetry (TRS) breaking phase in a small doping interval in the overdoped region when interlayer tunneling is strong enough. Contrary to expectations, being closer to the 45° twist angle does not expand this TRS region compared to a previous study [1] on a 53° twist angle. This is attributed to the fact that the two superconducting states in competition have almost identical nodal structures.

## I. INTRODUCTION

The observation of unconventional superconductivity in twisted bilayer graphene [2, 3] has motivated similar studies on various van der Waals heterostructures [4], like twisted boron nitride [5] and transition metal dichalcogenides [6–13]. Those systems offer more degree of freedom than their monolayer counterparts due to the twist angle that can be changed.

The realization of a two-dimensional monolayer of  $\text{Bi}_2\text{Sr}_2\text{CaCu}_2\text{O}_{8+\delta}$  (Bi2212) [14, 15] has motivated research on twistronics in cuprates [1, 16–19]. It has been predicted that a fully gapped  $d_{x^2-y^2} + id_{xy}$  superconducting phase emerges in systems with large twist angle close to 45° [16]. Spontaneous time-reversal symmetry (TRS) breaking is also predicted in this system and the superconducting phase is predicted to be topologically nontrivial. Chiral topological superconductivity is also predicted in twisted multilayer nodal superconductors [20].

The bilayer cuprate systems are natural Josephson junctions. Realizing those junctions in the laboratory is challenging due to disorder that may be introduced while preparing the sample [21, 22]. An early study of a c-axis cuprate Josephson junction did not show the *d*-wave behavior expected from cuprates [23]. New processes have been proposed to create those junctions and offer evidence that the Josephson current is reduced close to 45° due to a mismatch between the *d*-wave states of the two layers [21, 22, 24]. The critical current might remain finite at 45°, pointing to a state with TRS breaking [25]. Such behavior has been predicted using simple models describing twisted bilayer cuprates [26, 27].

Previous theoretical work based on Bogoliubov-de-Gennes mean-field theory lacks the effect of strong correlation, which are important in cuprate-based system. Moreover, the physics of cuprates is strongly doping dependent, being affected by the pseudogap phenomenon below optimal doping [28]. A twisted  $t-J$  model of cuprates within slave-boson mean field theory predicts that the range of twist angle around 45° which allows TRS breaking is narrow [29]. To address the effect of the strong correlation and the effect of doping, a Hubbard model for a system with a twist angle of  $\theta = 53.13^\circ$  has been studied with the vari-

ational cluster approximation (VCA) and cluster dynamical mean field theory (CDMFT) [1]. The TRS breaking was observed near optimal doping when strong interlayer tunneling was considered. It was conjectured that at a twist angle closer to 45°, the mixed state could be more stable as a function of doping. The number of orbitals per unit cell in systems close to 45° makes them challenging to study using quantum cluster methods.

In this paper we take a step further into studying systems close to 45°, by considering a Hubbard model for bilayer cuprates at a twist angle  $\theta = 43.60^\circ$ , corresponding to a unit cell of 58 copper sites. We use the VCA to probe the stability of the TRS-breaking superconducting phase against doping. We follow the methodology proposed in Ref. [1] and show that a TRS-breaking phase occurs in a narrow doping range, which can be explained by the band structure limiting the energy gained from combining the two superconducting states in competition.

## II. MODEL

We use the tight-binding Hubbard model proposed in Ref. [1], where each layer is described by a one-band Hubbard model, each site corresponding to a copper atom. The Hamiltonian can be separated as

$$H = H^{(1)} + H^{(2)} + H_\perp, \quad (1)$$

where the intralayer Hamiltonian  $H^{(l)}$  is

$$H^{(l)} = \sum_{\mathbf{r}, \mathbf{r}' \in l, \sigma} t_{\mathbf{r}\mathbf{r}'} c_{\mathbf{r}, l, \sigma}^\dagger c_{\mathbf{r}', l, \sigma} + U \sum_{\mathbf{r}} n_{\mathbf{r}, l, \uparrow} n_{\mathbf{r}, l, \downarrow} - \mu \sum_{\mathbf{r}, \sigma} n_{\mathbf{r}, l, \sigma} \quad (2)$$

where  $c_{\mathbf{r}, l, \sigma}$  ( $c_{\mathbf{r}, l, \sigma}^\dagger$ ) is the annihilation (creation) operator of an electron at site  $\mathbf{r}$  on layer  $l$  ( $l = 1, 2$ ) with spin  $\sigma = \uparrow, \downarrow$ , and  $n_{\mathbf{r}, l, \sigma}$  is the number operator.  $\mathbf{r}, \mathbf{r}'$  are the site indices of a square lattice for each layer.  $U$  is the on-site repulsion between electrons and  $t_{\mathbf{r}\mathbf{r}'}$  is the hopping matrix that includes nearest-neighbor hopping ( $t$ ) and next-nearest-neighbor hopping ( $t'$ ). In Bi2212, the nearest-neighbor hopping is  $t = 126$  meV [30], but here we are using  $t$  as

the energy unit. To describe Bi2212 we use the set of parameters  $t = 1$ ,  $t' = -0.3$  and  $U = 8$  [1, 30].

The effect of the twist angle comes from the interlayer tunneling given by

$$H_{\perp} = \sum_{n=1}^7 V_n \sum_{\langle \mathbf{r}, \mathbf{r}' \rangle_{\perp, n, \sigma}} [c_{\mathbf{r}, 1, \sigma}^{\dagger} c_{\mathbf{r}', 2, \sigma} + \text{H.c.}], \quad (3)$$

with  $\langle \mathbf{r}, \mathbf{r}' \rangle_{\perp, n, \sigma}$  representing the set of sites  $\mathbf{r}$  on layer 1 and  $\mathbf{r}'$  on layer 2 such that their projection on the plane are  $n$ th neighbors. We consider interlayer hopping up to 7th interlayer neighbors. The strength of the tunneling is given by

$$V_n = V e^{-\lambda(|\mathbf{d}_n| - d_z)/a}, \quad (4)$$

where  $|\mathbf{d}_n| = |\mathbf{r} - \mathbf{r}'|$  is the three-dimensional distance between the two sites corresponding to the  $n$ th neighbors on different layers,  $d_z$  is the distance between the two layers and  $a$  is the lattice constant of the square lattice.  $V$  is the interlayer tunneling of sites that are on top of each other.  $\lambda$  is a damping parameter. To have a set of parameters similar to the one used in Ref. [1], we chose  $d_z = a$  and  $\lambda = 11.13$  with two different values of  $V$ : 0.2 and 0.4.

This model is a simplification of the real situation in bilayer cuprates. The effect of the rare-earth layer in between the  $\text{CuO}_2$  plane is doubtless more complex. The model also neglects the fact that each monolayer of Bi2212 contains two  $\text{CuO}_2$  planes. The value of the interlayer tunneling parameters chosen here are very strong and should likely be lower in order to better describe real twisted bilayers. The strong values are needed to observe TRS breaking in our system [1].

In this work we consider a system with a twist angle  $\theta = 43.60^\circ$  to probe the TRS breaking close to the optimal twist angle. At this twist angle, the unit cell of the bilayer system contains 58 sites. To probe the superconducting phase in this model, we use the VCA [31, 32] with an exact diagonalization solver at zero temperature. This variational method on the electron self-energy based of Potthoff's self-energy functional approach allows us to probe broken symmetries while preserving strong correlations. It has been used to predict magnetic phases [32, 33] and superconductivity [13, 34] in various systems. For a detailed review of the method, see Refs [1, 35, 36].

The use of exact diagonalization limits the total number of orbitals in a cluster to about 12 because of the computational resources needed to compute the Green functions. Considering this, we need to separate the 58-site unit cell in clusters of smaller sizes. We separated our unit cell into 6 clusters as shown in Fig. 1: one cluster of two sites, one cluster of eight sites and four clusters of 12 sites each. This separation is not the only one possible, but it is one where every cluster but  $C$  contain full plaquettes from each layer. From experience, having full plaquettes stabilizes the superconducting phase in the single-layer problem.

The  $d$ -wave superconductivity operator on layer  $l$  is given

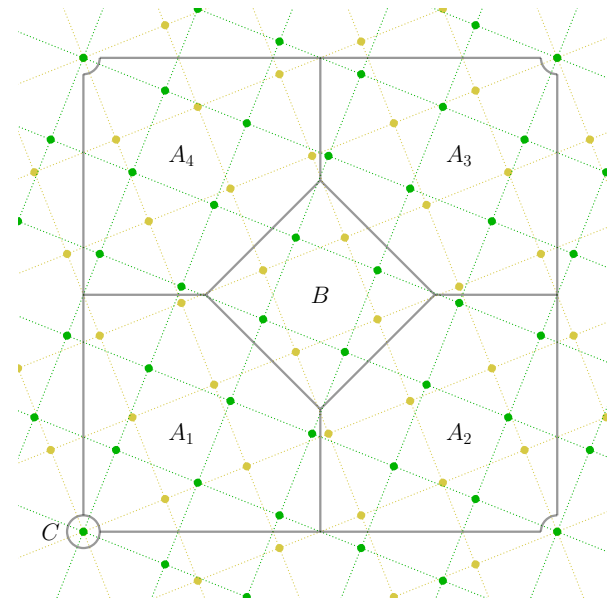


Figure 1. Unit cell of the twisted cuprate system at  $\theta = 43.60^\circ$ . It contains 58 sites between the two layers (green and yellow). The four  $A_i$  clusters contain 12 sites (6 from each layer), the  $B$  cluster contains 8 sites and the  $C$  cluster contains only 2 sites that are on top of each other.

by

$$\hat{\Delta}^{(l)} = \sum_{\mathbf{r} \in l} c_{\mathbf{r}, l, \uparrow}^{\dagger} c_{\mathbf{r} + \mathbf{x}^{(l)}, l, \downarrow} - c_{\mathbf{r}, l, \downarrow}^{\dagger} c_{\mathbf{r} + \mathbf{x}^{(l)}, l, \uparrow} - c_{\mathbf{r}, l, \uparrow}^{\dagger} c_{\mathbf{r} + \mathbf{y}^{(l)}, l, \downarrow} + c_{\mathbf{r}, l, \downarrow}^{\dagger} c_{\mathbf{r} + \mathbf{y}^{(l)}, l, \uparrow}, \quad (5)$$

where  $\mathbf{x}^{(l)}$  and  $\mathbf{y}^{(l)}$  are the lattice vectors on layer  $l$ .

From general principles we expect the superconducting order parameter to belong to either the  $B_1$  or the  $B_2$  representation of the  $D_4$  point group [1]. This corresponds to  $d$ -wave superconductivity in each layer, but with different relative signs:

$$\hat{B}_1 = \hat{\Delta}^{(1)} + \hat{\Delta}^{(2)}, \quad \hat{B}_2 = \hat{\Delta}^{(1)} - \hat{\Delta}^{(2)}. \quad (6)$$

These pairing operators are schematically illustrated on Fig. 2. We use the convention from Ref. [1], where the links with the same sign in the  $B_1$  representation are separated by the large angle ( $90^\circ - \theta = 46.4^\circ$ ). In the  $B_2$  representation, the links with the same sign are separated by the smaller angle ( $43.6^\circ$ ). At  $45^\circ$ , the two representations are equivalent and should correspond to degenerate states. The same if true if the inter-layer hopping  $V$  vanishes.

Both the  $B_1$  and  $B_2$  states are possible but one will generally have a lower energy, depending on doping. In the TRS-breaking phase, the two states are close in energy, and the complex combination  $B_1 + iB_2$  lowers the energy further. To probe the TRS-breaking superconducting phase, we use both the  $B_1$  and  $B_2$  representations simultaneously as Weiss fields in the VCA procedure and look for regions of

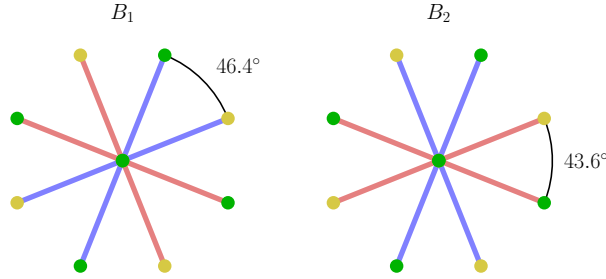


Figure 2. Schematics of the pairing operators associated with the  $B_1$  and  $B_2$  representations around the pivotal sites (C cluster from Fig. 1). The green (yellow) sites correspond to the top (bottom) layer. Positive (negative) pairing is represented by blue (pink) segments. In the  $B_1$  representation, the links with the same sign are separated by the larger angle ( $46.4^\circ$ ). In the  $B_2$  representation, they are separated by the smaller angle ( $43.6^\circ$ ).

doping where both are present in a complex linear combination,  $B_1 + iB_2$ . The Weiss field used in the VCA procedure was taken to be the same on all clusters. Using different Weiss fields on different clusters did not improve the results significantly and considerably increased the computational resources needed.

The order parameter  $\psi_{B_i}$  is defined as the average of the pairing operator per site

$$\psi_{B_i} = \frac{1}{L} \langle \hat{B}_i \rangle, \quad (7)$$

where  $L$  is the number of sites in the cluster (here 58) and  $i = 1, 2$ . In the case of a complex combination  $\psi_{B_1} + i\psi_{B_2}$ , the order parameter is given by the norm,  $|\psi_{B_1} + i\psi_{B_2}|$ . In this case, we can define a relative phase

$$\tan \frac{\phi}{2} = \frac{\text{Im} \psi_{B_2}}{\text{Re} \psi_{B_1}} \quad (8)$$

which corresponds to the phase difference between the  $d$ -wave operators of each layer, i.e., between  $\langle \hat{\Delta}^{(1)} \rangle$  and  $\langle \hat{\Delta}^{(2)} \rangle$ . A value of  $\phi = 0$  ( $\phi = \pi$ ) corresponds to a pure  $B_1$  ( $B_2$ ) case. TRS breaking occurs when  $\phi \neq 0$  or  $\pi$ .

We note that interlayer pairing occurs naturally when either layer is in the superconducting phase. We did not use interlayer pairing as an additional Weiss field since it has been shown that its addition does not increase the confidence in the solution while increasing the computational time and resources needed [1].

### III. RESULT AND DISCUSSION

We start by probing the superconducting phase in model (1) with  $\theta = 43.60^\circ$ , for types  $B_1$  and  $B_2$  separately. We can compare the energies of the two states and find a doping region where TRS breaking is likely to occur.

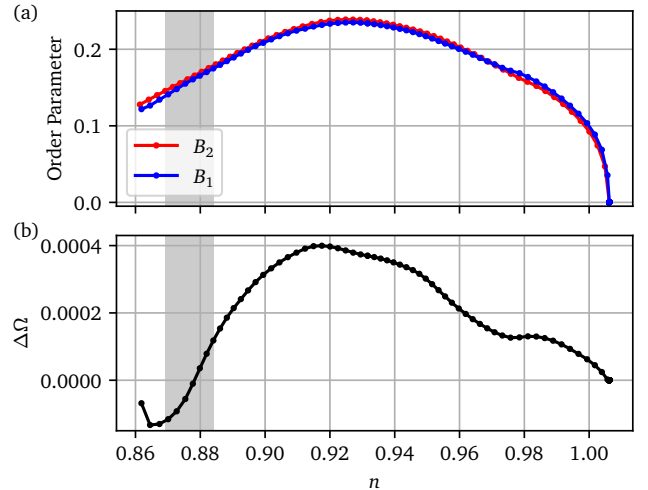


Figure 3. (a) : Norm of the order parameters obtained from the VCA procedure with a Weiss field belonging either to the  $B_1$  or  $B_2$  representation, for an interlayer hopping of  $V = 0.4$ , as a function of electron density  $n$ . (b) : Free energy difference  $\Delta\Omega$  between the two states (in units of  $t$ ). When  $\Delta\Omega > 0$  ( $\Delta\Omega < 0$ ) the  $B_1$  ( $B_2$ ) state is energetically favored. The grey region highlights the density range where a TRS breaking is observed (see text).

On Fig. 3 (a), we show the superconducting order parameter for the  $B_1$  and  $B_2$  states for  $V = 0.4$ . The two states have very similar superconducting domes. The order parameter vanishes around half-filling in both cases. That the order parameter does not vanish exactly at  $n = 1$  can be attributed to the error on the electron density typical of VCA when the chemical potential within the cluster is not treated as a variational parameter.

We can use the optimal value of the Potthoff functional in each state,  $\Omega_{B_1}$  and  $\Omega_{B_2}$ , as a measure of the free energy of the system [31]. In Fig. 3 (b), we show the difference  $\Delta\Omega = \Omega_{B_2} - \Omega_{B_1}$ . When  $\Delta\Omega$  is positive (negative) the  $B_1$  ( $B_2$ ) representation is energetically favored.

As shown in Fig. 3 (b), the difference  $\Delta\Omega$  for  $\theta = 43.60^\circ$  is of order  $10^{-4}$  (in unit of the nearest-neighbor hopping  $t$ ). For  $\theta = 53.13^\circ$ , the difference is more of order  $10^{-3}$  [1]. This is expected since at  $45^\circ$  the two representations should have the same energy. The closer the twist angle is to  $45^\circ$ , the closer in energy the states  $B_1$  and  $B_2$  should be and TRS breaking should be more likely. For  $V = 0.2$ , we obtained similar results with an even smaller  $\Delta\Omega$ , owing to the smaller interlayer tunneling.

We then probed the superconducting phase when both the  $B_1$  and  $B_2$  states are simultaneously allowed. The two representations can now compete against each other or combine into a combination  $B_1 + iB_2$ , whichever is energetically favorable. Fig. 4 shows the relative phase  $\phi$  computed using Eq. (8) as a function of the density  $n$  in a narrow range of density. For  $V = 0.2$ , it is possible to see an abrupt transition from the  $B_1$  state to the  $B_2$  state. The TRS-

breaking region is too narrow to be seen with our method. The three data points with non-zero  $\phi$  around  $n = 0.880$  may be an artifact caused by, e.g., the minimisation procedure, or the simplified Weiss field configuration used, with the same Weiss field on all clusters.

For  $V = 0.4$ , the relative phase shows a continuous transition from  $B_1$  to  $B_2$  upon increasing hole doping. We obtain a TRS-breaking state between  $n \approx 0.873$  and  $n \approx 0.881$ . The interlayer tunneling amplitude is the most important parameter controlling the mixing of the two representations, as noted previously [1].

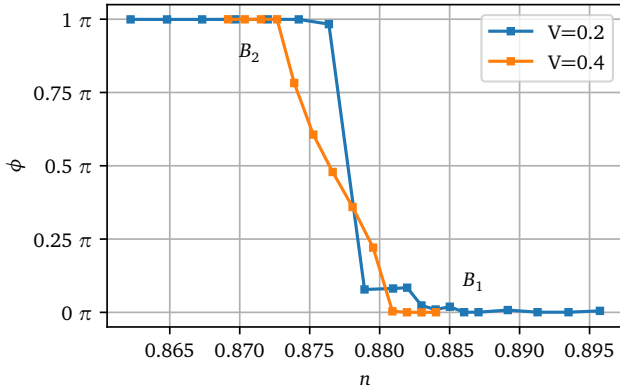


Figure 4. Relative phase  $\phi$  (Eq. (8)) as a function of  $n$ . We can observe a transition from  $B_1$  to  $B_2$  when doping is increased. For  $V = 0.4$ , a finite region of doping with  $\phi$  between 0 and  $\pi$  is observed, indicating a TRS-breaking phase. For  $V = 0.2$ , the width of this region, if it exists, is too small to be resolved.

The grey area in Fig. 3 highlights the region where TRS breaking is seen in Fig. 4 for  $V = 0.4$ . It is well beyond optimal doping and corresponds to the range of doping where  $\Delta\Omega$  is close to zero.

Our results are similar to those of Ref. [1], where a twist angle of  $\theta = 53.13^\circ$  was applied. A TRS-breaking phase near optimal doping was also observed in the strong interlayer regime. The TRS-breaking phase observed with  $\theta = 43.60^\circ$  occurs within a smaller doping range, in the overdoped region. It was expected that, closer to  $45^\circ$ , the TRS-breaking phase would occur in a wider doping range. This is not what we observe here.

To explain this, we turn to a simpler approach and consider, at  $U = 0$ , the effect of a mean field associated with each of the superconducting states  $B_1$  and  $B_2$  for  $\theta = 43.60^\circ$ . Usually we expect an energy gain when combining superconducting states from the same system if the nodes of each state are located at very different positions in the Brillouin zone (BZ). One example of this is the triplet state  $p_x + ip_y$ . This is not the case in twisted cuprates. One might think that combining a  $d$ -wave state from one layer with a  $d$ -wave from a second layer with a different orientation would effectively do the trick, but in fact this amounts to combining equivalent representations of two different systems instead of combining two different representations of

the same system. In reality, the representations  $B_1$  and  $B_2$  have nodes at the same place.

In Fig 5 (a) we show the band structure of Model (1) along the diagonal of the BZ for a non-zero  $B_1$  mean-field ( $b_1\hat{B}_1$ ,  $b_1 = 0.2$ ). For a twist angle of  $\theta = 43.60^\circ$  there are 58 bands and the BZ is folded 29 times. There are nodes in the vicinity of  $\mathbf{k} = (\pi/2, \pi/2)$  (same for the  $B_2$  state, not shown in panel (a)). On panel (b), we compare the band structures with  $B_1$  and  $B_2$  mean-fields around the node (note the enlarged scale). The nodes are not perfect and are in fact already gapped for both states: no linear combination  $B_1 + iB_2$  is needed to generate the gap. Indeed, when a system has multiple orbitals, the nodes are not necessarily fixed by symmetry [37]. Following this argument, the energy gained by a complex combination  $B_1 + iB_2$  can remain small even close to  $45^\circ$ . Hence, the twist angle should not be the only parameter affecting the extent of the TRS-breaking phase, nor indeed the most important one. Other parameters, like doping and disorder [38], may play a key role.

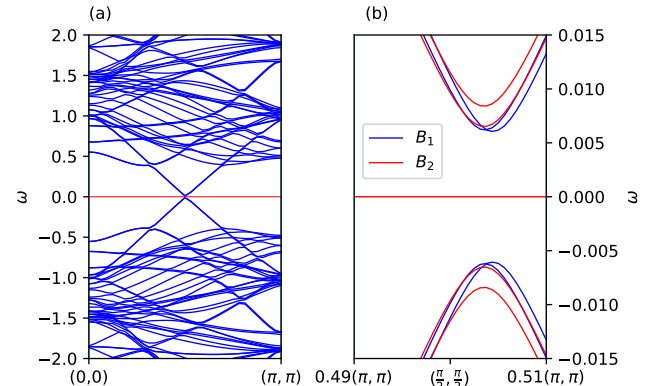


Figure 5. Band structure of model (1) with  $U = 0$  and a superconducting mean-field  $b_i\hat{B}_i$ . (a) Band structure along the diagonal of the first quadrant of the Brillouin zone for  $b_1 = 0.2$ . The nodes are located around  $\mathbf{k} = (\pi/2, \pi/2)$ . (b) Close-up of the region around the nodes for  $b_1 = 0.2$  (blue) and  $b_2 = 0.2$  (red). The nodes are in fact slightly gapped for both representations and very close to each other.

#### IV CONCLUSION

We used a one-band Hubbard model for twisted bilayer cuprates at  $\theta = 43.60^\circ$  with VCA to search for a possible TRS-breaking superconducting phase. In the twisted bilayer, superconductivity is expected away from half filling either in the  $B_1$  or  $B_2$  representation of the  $D_4$  point group. We found that a phase transition from the  $B_1$  state to the  $B_2$  state when doping is increased. A region where the complex combination  $B_1 + iB_2$  is stable, thus breaking TRS, occurs in a small range of doping when the interlayer doping is strong enough. Our results are in accord with previous

work on the  $53.13^\circ$  system, where the observation of TRS breaking needed a strong interlayer tunneling [1]. We also show that the two states  $B_1$  and  $B_2$  are closer in energy when the twist angle approaches  $45^\circ$ , where they are expected to be equivalent.

The energy difference between the two states being smaller as the twist angle approaches  $45^\circ$  makes it harder to probe TRS breaking. With a simple mean-field argument, we show that the nodes of the  $B_1$  and  $B_2$  states are very close, making the energy gain from combining them very small. Hence, the twist angle cannot be the only parameter controlling the TRS breaking. The doping level needs to be considered, alongside the twist angle and probably disorder level, to create a robust TRS-breaking state.

The system studied here is made of two layers of the same cuprate model, with the same doping. Taking in-

spiration from the heterobilayer transition metal dichalcogenides [6, 12], layers of different cuprates might be used to stabilize the TRS-breaking state. The difference in doping and structure might lead to a change in the TRS-breaking region. We will address this question in a future work.

## ACKNOWLEDGMENTS

This work was supported by the Natural Sciences and Engineering Research Council of Canada (NSERC) under grant RGPIN-2020-05060, by the NSERC postgraduate scholarships doctoral program and by the *Fonds de Recherche du Québec Nature et technologies* (FRQNT) doctoral research scholarships. Computational resources were provided by the Digital Research Alliance of Canada and Calcul Québec.

---

[1] X. Lu and D. Sénéchal, *Phys. Rev. B* **105**, 245127 (2022).

[2] Y. Cao, V. Fatemi, A. Demir, S. Fang, S. L. Tomarken, J. Y. Luo, J. D. Sanchez-Yamagishi, K. Watanabe, T. Taniguchi, E. Kaxiras, R. C. Ashoori, and P. Jarillo-Herrero, *Nature* **556**, 80 (2018).

[3] Y. Cao, V. Fatemi, S. Fang, K. Watanabe, T. Taniguchi, E. Kaxiras, and P. Jarillo-Herrero, *Nature* **556**, 43 (2018).

[4] L. Balents, C. R. Dean, D. K. Efetov, and A. F. Young, *Nat. Phys.* **16**, 725 (2020).

[5] L. Xian, D. M. Kennes, N. Tancogne-Dejean, M. Altarelli, and A. Rubio, *Nano Lett.* **19**, 4934 (2019).

[6] D. A. Ruiz-Tijerina and V. I. Fal'ko, *Phys. Rev. B* **99**, 125424 (2019).

[7] L. Wang, E.-M. Shih, A. Ghiotto, L. Xian, D. A. Rhodes, C. Tan, M. Claassen, D. M. Kennes, Y. Bai, B. Kim, K. Watanabe, T. Taniguchi, X. Zhu, J. Hone, A. Rubio, A. N. Pasupathy, and C. R. Dean, *Nat. Mater.* **19**, 861 (2020).

[8] L. An, X. Cai, D. Pei, M. Huang, Z. Wu, Z. Zhou, J. Lin, Z. Ying, Z. Ye, X. Feng, R. Gao, C. Cacho, M. Watson, Y. Chen, and N. Wang, *Nanoscale Horiz.* **5**, 1309 (2020).

[9] Z. Zhang, Y. Wang, K. Watanabe, T. Taniguchi, K. Ueno, E. Tuttuc, and B. J. LeRoy, *Nat. Phys.* **16**, 1093 (2020).

[10] S. Venkateswarlu, A. Honecker, and G. Trambly de Laisardi  re, *Phys. Rev. B* **102**, 081103 (2020).

[11] E. C. Regan, D. Wang, C. Jin, M. I. Bakti Utama, B. Gao, X. Wei, S. Zhao, W. Zhao, Z. Zhang, K. Yumigeta, M. Blei, J. D. Carlstr  m, K. Watanabe, T. Taniguchi, S. Tongay, M. Crommie, A. Zettl, and F. Wang, *Nature* **579**, 359 (2020).

[12] Y. Tang, L. Li, T. Li, Y. Xu, S. Liu, K. Barmak, K. Watanabe, T. Taniguchi, A. H. MacDonald, J. Shan, and K. F. Mak, *Nature* **579**, 353 (2020).

[13] M. B  langer, J. Fournier, and D. S  n  chal, *Phys. Rev. B* **106**, 235135 (2022).

[14] Y. Yu, L. Ma, P. Cai, R. Zhong, C. Ye, J. Shen, G. D. Gu, X. H. Chen, and Y. Zhang, *Nature* **575**, 156 (2019).

[15] S. Y. F. Zhao, N. Poccia, M. G. Panetta, C. Yu, J. W. Johnson, H. Yoo, R. Zhong, G. D. Gu, K. Watanabe, T. Taniguchi, S. V. Postolova, V. M. Vinokur, and P. Kim, *Phys. Rev. Lett.* **122**, 247001 (2019).

[16] O. Can, T. Tummuru, R. P. Day, I. Elfimov, A. Damascelli, and M. Franz, *Nat. Phys.* **17**, 519 (2021).

[17] P. A. Volkov, J. H. Wilson, K. P. Lucht, and J. H. Pixley, *Phys. Rev. B* **107**, 174506 (2023).

[18] G. Margalit, B. Yan, M. Franz, and Y. Oreg, *Phys. Rev. B* **106**, 205424 (2022), arXiv:2209.11080 [cond-mat].

[19] A. Mercado, S. Sahoo, and M. Franz, *Phys. Rev. Lett.* **128**, 137002 (2022).

[20] T. Tummuru, E. Lantagne-Hurtubise, and M. Franz, *Phys. Rev. B* **106**, 014520 (2022).

[21] M. Martini, Y. Lee, T. Confalone, S. Shokri, C. N. Saggau, D. Wolf, G. Gu, K. Watanabe, T. Taniguchi, D. Montemurro, V. M. Vinokur, K. Nielsch, and N. Poccia, “Twisted cuprate van der Waals heterostructures with controlled Josephson coupling,” (2023), arXiv:2303.16029 [cond-mat].

[22] Y. Lee, M. Martini, T. Confalone, S. Shokri, C. N. Saggau, D. Wolf, G. Gu, K. Watanabe, T. Taniguchi, D. Montemurro, V. M. Vinokur, K. Nielsch, and N. Poccia, *Advanced Materials* **35**, 2209135 (2023).

[23] Y. Zhu, M. Liao, Q. Zhang, H.-Y. Xie, F. Meng, Y. Liu, Z. Bai, S. Ji, J. Zhang, K. Jiang, R. Zhong, J. Schneeloch, G. Gu, L. Gu, X. Ma, D. Zhang, and Q.-K. Xue, *Phys. Rev. X* **11**, 031011 (2021).

[24] J. Lee, W. Lee, G.-Y. Kim, Y.-B. Choi, J. Park, S. Jang, G. Gu, S.-Y. Choi, G. Y. Cho, G.-H. Lee, and H.-J. Lee, *Nano Lett.* **21**, 10469 (2021).

[25] S. Y. F. Zhao, N. Poccia, X. Cui, P. A. Volkov, H. Yoo, R. Engelke, Y. Ronen, R. Zhong, G. Gu, S. Plugge, T. Tummuru, M. Franz, J. H. Pixley, and P. Kim, “Emergent Interfacial Superconductivity between Twisted Cuprate Superconductors,” (2021), arXiv:2108.13455 [cond-mat].

[26] P. A. Volkov, S. Y. F. Zhao, N. Poccia, X. Cui, P. Kim, and J. H. Pixley, “Josephson effects in twisted nodal superconductors,” (2021), arXiv:2108.13456 [cond-mat].

[27] T. Tummuru, S. Plugge, and M. Franz, *Phys. Rev. B* **105**, 064501 (2022).

[28] S. S. Dash and D. S  n  chal, *Phys. Rev. B* **100**, 214509 (2019).

[29] X.-Y. Song, Y.-H. Zhang, and A. Vishwanath, *Phys. Rev. B* **105**, L201102 (2022).

[30] R. S. Markiewicz, S. Sahrakorpi, M. Lindroos, H. Lin, and A. Bansil, *Phys. Rev. B* **72**, 054519 (2005).

[31] M. Potthoff, M. Aichhorn, and C. Dahnken, *Phys. Rev. Lett.* **91**, 206402 (2003).

[32] C. Dahnken, M. Aichhorn, W. Hanke, E. Arrigoni, and M. Potthoff, *Phys. Rev. B* **70**, 245110 (2004).

[33] P. Sahebsara and D. Sénéchal, [Phys. Rev. Lett. \*\*100\*\*, 136402 \(2008\)](#).

[34] J. P. L. Faye and D. Sénéchal, [Phys. Rev. B \*\*95\*\*, 115127 \(2017\)](#).

[35] M. Potthoff, in *Strongly Correlated Systems: Theoretical Methods*, Vol. 171, edited by A. Avella and F. Mancini (Springer Berlin Heidelberg, Berlin, Heidelberg, 2012) pp. 303–339.

[36] M. Potthoff, in *DMFT: From Infinite Dimensions to Real Materials*, Vol. 8, edited by E. Pavarini, E. Koch, A. Lichtenstein, and D. Vollhardt (Forschungszentrum Jülich, 2018) pp. 5.1–5.33.

[37] S.-O. Kaba and D. Sénéchal, [Phys. Rev. B \*\*100\*\*, 214507 \(2019\)](#).

[38] A. C. Yuan, Y. Vituri, E. Berg, B. Spivak, and S. A. Kivelson, “[Inhomogeneity-Induced Time-Reversal Symmetry Breaking in Cuprate Twist-Junctions](#),” (2023), arXiv:2305.15472 [cond-mat].